A SPECTROSCOPIC ANALYSIS OF THE INTERACTION BETWEEN MEGA10 AND CONCANAVALIN A

J.A. Molina-Bolívar[1*], C. Carnero Ruiz[1], F. Galisteo-González[2], A. Aguilera-Garrido[2], M.J. Gálvez-Ruiz[2]

[1]*Department of Applied Physics II and Excellence Research Unit "Modeling Nature" (MNat), Engineering School, University of Málaga, 29071 Málaga, Spain*

[2]*Department of Applied Physics and Excellence Research Unit "Modeling Nature" (MNat), University of Granada, 18071 Granada, Spain*

[*]Corresponding author:

J.A. Molina Bolívar

Departamento de Física Aplicada II

Universidad de Málaga.

Campus de Teatinos

29071 – Málaga, Spain

jmb@uma.es

Abstract:

The binding of MEGA10 with Concanavalin A (Con A) at pH 7.4 and pH 5 have been studied using steady-state and time-resolved fluorescence, dynamic light scattering (DLS) and Circular Dichroism (CD). Downward curving Stern-Volmer plots suggested the existence of tryptophan residues exposed in the protein surface and other tryptophans extensively buried within the protein. The major proportion of protein tryptophan groups are not involved in MEGA10 interaction. The pH significantly influences the affinity of MEGA10 to Con A, with it being stronger at pH 7.4 than at pH 5.0. It is inferred from the thermodynamic analysis of the binding constant dependence with temperature that van der Waals and hydrogen bonds are the predominant forces in the interaction of MEGA10 with lectin. In time-resolved fluorescence experiments, the decay curves were well fitted to three exponential patterns. The mean lifetime at pH 7.4 systematically decreased with increasing MEGA10 concentration, whereas this parameter at pH 5 is practically constant, indicating greater protein structure alterations at pH 7.4 than at pH 5 after surfactant association, and they were corroborated by circular dichroism measurements. Anisotropy complementary studies detail that Con A undergoes motion restrictions because of the association with surfactant. The attachment of MEGA10 to Con A was confirmed by dynamic light scattering.

Keywords: MEGA10, Con A, quenching fluorescence, lifetimes, thermodynamic study

Highlights

- The interaction between MEGA10 and Con A was studied at different temperature and pH values
- Hydrogen bonds and van der Waals forces are predominant interactions
- Conformational changes of the protein upon binding of MEGA10 were observed

1. Introduction

Nano and microparticles offer multiple possibilities in the advancing of medicine, providing solutions to problems that cannot be solved with standard medical approaches [1]. Research and innovation in nanomedicine tackles many aspects, such as the development of biosensors, diagnosis devices, vaccines or carriers for chemotherapeutic agents. Modern cancer treatments with drugs often present the disadvantage of killing healthy cells. Therefore, it is desirable to develop effective targeted therapies for the selective destruction of cancerous tissue [2]. In this context, nanoparticles have emerged as a promising alternative to improve the therapeutic index of drugs by increasing their targeting capacity and accumulation in specific organs, tissues or cells while decreasing potential toxicity and any adverse effect. This goal can be achieved by passive or active targeting. The characteristic size of nanoparticles, below 1 μm, means they can be passively accumulated in tumoral tissues by means of the enhanced permeability and retention effect (EPR) [3]. Active targeting is accomplished by nanocarrier binding specifically to characteristic receptors on cancerous cell. Several mechanisms and strategies have been proposed to improve selective binding of nanoparticles to the specific site. The functionalization of nanocarriers using targeting ligands such as monoclonal antibodies, peptides fragments, folate, surfactants and carbohydrates deserved special attention [4,5,6]. In recent years, there has been growing interest in the use of carbohydrates-sensibilized nanoparticles that can be used to specifically bind lectin, a protein overexpressed on the surface of numerous cancer cells [7,8,9]. On the other hand, lectin-mediated drug targeting also include nanoparticles decorated with lectin for specific binding to sugar on the wall of diseased cells. Cancerous cells express different glycans compared with their normal counterparts [10]. A well characterization of interaction between lectin and carbohydrate is fundamental for both approaches in order

to accomplish high selectivity and sensibility [11]. It is accepted in literature that higher binding affinity increases targeting efficacy [2].

Surfactants derived from carbohydrates (sugar-based surfactants) are nonionic amphiphiles characterized by having a hydrophobic alkyl chain linked to a sugar residue. These surfactants have increasingly become of interest owing to their excellent biodegradability, nontoxicity and availability from renewable sources [12]. Different nanoparticles synthetized from sugar-based surfactants have been examined as drug carriers [13,14]. Hashim *et al.* prepared vesicles formulated with octyl glucoside and maltoside [15]. *In vitro* release of methotrexate encapsulated in niosomes prepared from alkyl glucopyranoside surfactants was studied by La Mesa *et al* [16]. Sugar-based surfactants are incorporated into liposomes to increase their resistance to macrophages. An important class of the aforementioned surfactant group are the fatty acid glucamides, whose most relevant member is N-decanoyl-N-methylglucamide (MEGA10) which has been widely used as a membrane protein solubilizer as this amphiphile seems to preserve the protein functions [17,18].

The above considerations prompted us to investigate the interaction of Concanavalin A (Con A) with MEGA10 with the aim of using this sugar-based surfactant as ligand for the targeted delivery of anticancer drugs. Fluorescence spectroscopic techniques in connexion with DLS and CD measurements were used to characterize the association process. Concanavalin A, a lectin extracted from the *Canavalia ensiformis* (Jack bean) plant, is extensively used to describe carbohydrate-lectin binding. Con A is frequently used to distinguish normal and tumor cell membrane which experiments glycosylation processes [19]. This protein is dimeric or tetrameric, depending on the pH, whose subunits present high structural similarity. Each monomeric Con A contains 4 tryptophans and 7 tyrosines residues[20].

2. Experimental

2.1. Materials

Concanavalin A (Con A) from Jack bean and MEGA10 were commercially supplied by Sigma Aldrich (Madrid, Spain). These compounds were used as received. The molecular weight of Con A monomer is 26.5 kDa. Ultrapure water (resistivity ~18 MΩ·cm), used to prepare all the solutions, was obtained in a Milli-Q Academic Millipore system. The pH of working solutions, used immediately after preparation, was controlled with buffers (acetate at pH 5 and phosphate at pH 7).

2.2. Instruments and spectral measurements

All steady-state fluorescence measurements were performed on a FluoroMax-4 (Horiba, Jobin Yvon) spectrofluorometer, equipped with a 150-W xenon lamp and a cell housing with 1.0-cm path-length quartz cuvettes, which was thermostated by a Peltier unit. Concanavalin A solutions were irradiated at 295 nm to selectively excite tryptophan residues of the protein and emission spectra were scanned from 300 to 500 nm with an integration time of 0.1 s and slit widths for excitation and emission of 2 and 4 nm, respectively. Fluorescence intensities were collected at the wavelength corresponding to the emission maximum (339 nm) of the protein. In fluorescence quenching experiments, a volume of 2 ml of Con A at 12 μM was titrated by successive additions of small volumes of a solution of MEGA10 at 9.8 mM. The addition was performed manually using a micro syringe.

Fluorescence lifetimes of Con A in the absence and presence of MEGA10 were determined from time-resolved fluorescence measurements. The LifeSpec II luminescence spectrometer (Edinburgh Instruments), equipped with a 295 nm pulsed

light-emitting diode and a pulse of 100 ns, with emission being recorded at 340 nm, was used for this purpose. Data analysis was performed using the FAST software package from Edinburgh Instruments. The instrumental response function (IRF) was regularly obtained by measuring the scattering of a Ludox solution. Triexponential functions were used to fit the fluorescence decays, and the fit goodness was evaluated by χ^2 values and visual inspection of residuals. Average fluorescence lifetimes (τ) were calculated from the three-component contributions using the following equation:

$$\tau = \frac{\sum_{i=1}^{3} A_i \, \tau_i^2}{\sum_{i=1}^{3} A_i \tau_i} \quad (1)$$

where A_i is a pre-exponential factor for the component i with a lifetime τ_i. The relative concentration, or fractional amount of each component (α_i), was determined by:

$$\alpha_i = \frac{A_i}{\sum_i A_i} \quad (2)$$

The alterations of Con A conformation in the presence of MEGA10 were measured by far-UV (200–260 nm) circular dichroism (CD) measurements using a J-810 CD spectrometer (JASCO, Japan) at room temperature under a nitrogen atmosphere with a slit width of 1 nm. Each spectrum represented the average of five consecutive scans with a scan speed of 50 nm/min at 0.2 nm intervals, using a 2 mm quartz cell. The Con A concentration was kept constant at 11 μM while MEGA10 concentration was 100 μM. The solvent spectrum obtained under the same conditions was subtracted to obtain the actual sample spectrum. The CD raw data, received in terms of ellipticity (θ_{obs}), were transformed to mean residue ellipticities (MRE in deg cm^2 dmol^{-1}) using Equation [21]:

$$MRE = \frac{\theta_{obs}}{10 n c l} \quad (3)$$

where *n* is the number of amino acid residues (237 for Con A monomer), *c* is the Con A molar concentration and *l* is the path length of the cuvette in cm. Dynamic light scattering is frequently used to determine the hydrodynamic size of nanoparticles. A ZetaSizer Nano-S (Malvern Instrument, UK) apparatus was used to obtain the hydrodynamic radius of Con A in the presence of MEGA10.

3. Results and discussion

3.1. Steady-state fluorescence and binding constants

Fluorescence spectroscopy is a powerful technique that has been often used to investigate the binding of small molecules to proteins. This technique is very sensitivity towards the perturbation of the local environment of fluorophores [22]. The interaction of ligand with protein induces an increasing exposition of fluorophores to a more hydrophilic environment changing the fluorescence of the native protein. Tryptophan (Trp) residues have a high quantum yield in hydrophobic environment; in contrast, their quantum yield decreases in a hydrophilic medium. Concanavalin A (Con A) exists as tetrameric structure at pH>7 and as a dimer at pH 5, where each monomer has a binding site for carbohydrates. Trp residues are responsible for the fluorescence emission spectra of Con A when excited at 295 nm. Figs 1A and 1B show the fluorescence quenching of Con A in the presence of increasing concentrations of MEGA10 at neutral and acid pHs, respectively. The existence of quenching suggests that MEGA10 binds to Con A. The binding of MEGA10 to protein alters the microenvironment of Trp residues, thereby inducing the alteration of the intrinsic fluorescence of Con A. It is noteworthy that the extent of quenching by the surfactant at pH 7.4 is higher than at pH 5. The absence of relevant changes in the wavelength of maximum emission of Con A suggests that any

conformational changes resulting from surfactant binding do not lead to major exposure of lectin tryptophan groups to the aqueous environment. The fluorescence emission maximum occurs at 339 nm, showing that tryptophan amino acids are of Class II. This type of Trp residues corresponds to fluorophores exposed to the bound water with long dipole relation time [23].

Quenching data are recurrently presented as plots of the ratio between the fluorescence intensities in the absence and presence of quencher (I_0/I) versus concentration of quencher (the so-called Stern-Volmer plot) [24]. Figure 2 corresponds to the Stern-Volmer plot for Con A fluorescence quenching by MEGA10 in the two assayed media. Each point on the plot results from the average of three fluorescence intensity values measured at λ_{max}=339 nm. The profiles obtained show a nonlinear relationship and exhibits a sharp downward curvature. A linear Stern-Volmer plot is usually associated with the existence of a single class of tryptophan, all equally accessible to the quencher [25]. In the case of a protein with more than one type of tryptophanyl residues, the Stern-Volmer plot is not linear and the shape of the curve is characteristic of the relative degree of exposure of residues. In the particular case in which there are two tryptophan populations, one readily available to the quencher and one not, the plot deviates from linearity toward the x-axis. The observed result in our plot (Figure 2) is expected for a protein with a large number of Trp residues such as Con A, where tryptophanyl residues are in different surroundings and they are diversely accessible to surfactant. Similar upward curving profiles have been reported for other lectins [26-29].

The convex Stern-Volmer plot can be analyzed using the following equation [30-32]:

$$\frac{I_0}{I_0 - I} = \frac{1}{f_a} + \frac{1}{f_a K_Q [Q]} \qquad (4)$$

where K_Q is the effective quenching constant, f_a is the fraction of initial fluorescence that is accessible to quencher, and [Q] denotes the concentration of MEGA10 in molar. This equation allows the accessibility of Trp residues in Con A to MEGA10 to be estimated. Figure 3 shows the plot of $I_0/(I_0 - I)$ against $1/[MEGA{-}10]$ at pH 7.4 and pH 5 at 298 K. The intercept of the above curves yields f_a^{-1} for both pHs. The good linearity in the plots confirms the existence of both buried and exposed Trp residues in Con A. The f_a values thus obtained were 0.14 and 0.09 for pH 7.4 and pH 5, respectively. At both pHs, a small fraction of the emission of Con A is quenched by the surfactant, being the solvent accessibility of tryptophan residues higher at physiological pH. These results indicate that an important portion of tryptophanyl residues is not directly involved in surfactant binding, which cannot penetrate the protein matrix. Manda *et al*. suggested that most tryptophans of Con A are localized in a rigid environment, and hence buried and not exposure to solvent [33]. Considering the crystal structure of monomer Con A and fluorescence quenching by iodine ions, it has been postulated that only two (at 88 and 182) of the four Trp residues are close to the protein surface [34]. Probably tryptophan residues are away from the sugar-binding site of Con A.

The dependence of Con A fluorescence intensity on the MEGA10 concentration can be used to check the strength of the interaction between ligand and protein. The association constant (K_a) was determined using the Lineweaver-Burk equation at three temperatures (298 K, 305 K and 310 K) [35-37]:

$$\frac{1}{I_0 - I} = \frac{1}{I_0} + \frac{1}{I_0 K_a [Q]} \tag{5}$$

Thus, a linear plot of $1/\Delta I$ vs. $1/[Q]$, where $\Delta I = I_0 - I$, provides I_0 from the intercept on the ordinate, while the slope gives the estimate for the association constant. These plots are

presented in Figs 4A and 4B for pH 7.4 and pH 5, respectively. A good linearity (R^2>0.997) was observed. Table 1 collects the values of K_a . A large K_a value indicates strong interaction between MEGA10 and Con A. The association constant values for Con A-MEGA10 were found in the order of 10^3-10^4 M^{-1} for all studied temperatures, indicating moderate interaction. As a general trend, one can observe that protein-surfactant interaction is less favorable at higher temperatures. In addition, the association of MEGA10 to Con A is weaker at pH 5 than at pH 7.4, indicating that MEGA10 molecules bind to tetrameric form of Con A with greater affinity than to the dimeric structure. The values for K_a were found to bear good consistency with those reported in literature for other lectin-sugar interactions. For example, N-acetyl-lactosamine associates to the lectin obtained from the seed of *Moringa oleifera* or from *Dolichos lablab* with a binding constant of $1.38x10^3$ M^{-1} or $8.45x10^3$ M^{-1}, respectively [29, 31]. On the other hand, the association constant between Con A and N-acetyl glucosamine, or with α-D-glucopyranoside, is $3.48x10^4$ M^{-1} [38] and $1x10^4$ M^{-1} [39], respectively.

In general, the quenching between fluorophore and quencher arises due to static or dynamic interactions. They are distinguished based on their temperature dependence For static quenching, the rising temperature causes the instability of ligand-protein complex that in turn leads to a diminution in the quenching constant. To the contrary, the enhancement of diffusion coefficients with temperature in the dynamic quenching mechanism leads to an increase in the quenching constant. A comparison between Eqs 4 and 5 reveals the equivalence between K_Q and K_a. Inspection of the values of K_a in Table 1 indicates that quenching constant decreases, for both pHs, upon the temperature increasing. Higher temperature weakens the linking of Con A-MEGA 10 ground state

complex, resulting can therefore be inferred to be mainly due to a protein-surfactant assembly rather than dynamic collision.

3.2. Nature of the binding forces

The nature of binding forces is often characterized by the sign and magnitude of different thermodynamic parameters [24, 37]. Positive values of ΔS and ΔH is mostly indicative of hydrophobic interaction; while, specific electrostatic forces are characterized by positive ΔS and negative ΔH values. On the other hand, negative values for both thermodynamic parameters arise from van der Waals forces as well as hydrogen bond formation [40]. To calculate the thermodynamic parameters of Con A-MEGA 10 interaction, the following equations were used [24, 37]:

$$\Delta G^0 = -RT \ln K_a \tag{6}$$

$$\Delta H^0 = -T^2 \left[\frac{d\left(\Delta G^0 / T \right)}{dT} \right] \tag{7}$$

$$T\,\Delta S^0 = \Delta H^0 - \Delta G^0 \tag{8}$$

Thus, we calculated the ΔG^0 values by substituting the values of K_a in Eq. (6). We then estimated, from the slopes of the $\Delta G^0/T$ vs. T plots (see Figure 5), ΔH^0 by Eq. (7), and finally, the corresponding entropic contributions were calculated from Eq. (8). The thermodynamic functions calculated in this way are collected in Table 1. Spontaneity of the MEGA10 binding with lectin was elucidated by the evaluation of the Gibbs free energy change. The unfavourable negative entropy change values ($\Delta S^0 < 0$) can be compensated by the negative enthalpy change values ($\Delta H^0 < 0$), suggesting that the interaction is enthalpically driven. The binding of MEGA10 with Con A is

thermodynamically more favourable at physiological pH than at pH 5. According to the thermodynamic parameters, van der Waals forces and hydrogen bonds play the major role in the protein-surfactant interaction. It is worth noting that sugar-based surfactants possess a high hydrophilicity arising from the fact that each of their hydroxyl group can form as many as three hydrogen bonds in aqueous media [41]. This capability of MEGA10 to form hydrogen bonds is responsible for the linking with Con A. Con A binds to glucose and mannose residues that possess free hydroxyl groups at Positions 3, 4, and 6 of the α-pyranose ring through hydrogen bonds [42]. The heat release ($\Delta H^0 < 0$) could be due to the release of water molecules from lectin surface to bulk solution when hydrogen bonds are formed between the protein and the surfactant. The entropic loss of the system after the binding process could be related to the decrease in the motion freedom of MEGA10 upon the linking with the lectin.

The f ΔH^0 plots as a function of temperature are found to be linear (data not shown). The slope of these plots corresponds to the molar heat capacity change, ΔC_p. for the binding process. The values of ΔC_p calculated from linear regression analysis were -0.45 kJ/mol K and -0.37 kJ/mol K for pH 7.4 and pH 5, respectively. The negative slope signifies that the protein-surfactant association is more exothermic as the temperature increases. It is generally accepted that the main factor influencing the heat capacity for an association process is the solvent reorganization at the protein surface [43]. Negative ΔC_p corresponds to protein dehydration due to surfactant binding [37].

3.3. Time-resolved fluorescence studies

Time-resolved fluorescence can provide complementary information about the conformational changes of lectin upon surfactant addition. Figure 6A displays some typical examples of the fluorescence lifetime decay profiles corresponding to pure Con A and in the presence of 157 μM of MEGA10 at pH 7.4. The decay profiles in all cases

were adequately fitted by three-exponential functions ($\chi^2 \leq 1.07$). Table 2 collects the fluorescence lifetimes and the corresponding Con A weighting factors in absence and presence of MEGA10 at pH 7.4, whereas Table 3 presents the corresponding values for pH 5. The low values of χ^2 are convincing evidence for the three-exponential decay fitting. Multi-exponential decays are not surprising for multitryptophan proteins. Weighting factors (α_1, α_2 and α_3) depict the relative contributions of each component to the total fluorescence intensity. In the absence of surfactant at neutral pH, the longer component of 5.6 ns and the shorter one of 0.8 ns were measured. These components decreased at 4.6 ns and 0.7 ns, respectively, for pH 5. The observed differences could be attributed to protein structure alterations with pH, which affects the attachment capacity of MEGA10 to Con A. Interpretation of intensity decays is complicated for multitryptophan proteins. It is seducing to assign the various components to the individual tryptophan residues. However, even proteins with a single tryptophan residue typically display double or triple-exponential decays [24,25]. Hence, there is no reason to believe that the individual decay times represent individual Trp residues. Generally, buried Trp residues present shorter lifetimes, with the longer lifetimes being for exposed tryptophans [25]. Accordingly, as reflected in Tables 2 and 3, most Con A tryptophan residues are buried, in concordance with steady-state measurements.

Figure 6B illustrates the average lifetime as a function of MEGA10 concentration at both pHs. At pH 7.4, the mean lifetime decreased regularly with increasing MEGA10 concentration, whereas it is not altered significantly at pH 5. The binding of MEGA10 at pH 5 does not probably lead to any relevant structural changes in lectin. Turning our attention to the data in Tables 2 and 3, it should be noted that the three lifetime components for Con A decreased upon MEGA10 addition at physiological pH, whereas they did not practically vary in acid medium. The slight decrease in the weighting factor

of the buried Trp residues at pH 7.4 is noteworthy. In contrast, α_1 remains more or less unaffected at pH 5. Two explanations could be invoked to explain these results: (i) the binding of MEGA10 at pH 5 does not perturb the Trp environment significantly in opposite to pH 7.4; (ii) at pH 5 Trp residues are not present in the surfactant binding site of Con A. For both pHs, the value of α_3, which could correspond to the contribution of Trp residues exposed to water, increases as MEGA10 concentration rises.

3.4. Angular anisotropy and dynamic light scattering

We measured the steady-state anisotropy (r_{ss}) of lectin in the presence of increasing concentrations of surfactant (Figure 7) in order to gain insight into the interaction of Con A with MEGA10. This figure displays the successive increase of r_{ss}, which confirms that the association between MEGA10 and Con A occurs. The behaviour is similar at both pH values for MEGA10 concentrations below 40 µM. However, the anisotropy is greater at pH 7.4 than at pH 5 for higher surfactant concentrations, at the same MEGA10 concentration. Measurements of angular anisotropy of a protein make it possible to analyze the rotation of the protein molecule as a whole because Trp residues are not free to move [44]. When Con A experiences a restricted motion, an increase in anisotropy occurs that is indicative of conformational changes in the lectin structure.

Dynamic light scattering is a powerful tool for measuring the size of nanoparticles. Herein, this technique was used to investigate variations in the hydrodynamic radius of protein-surfactant complexes (R_H) with the concentration of MEGA10 (see Figure 8). This figure reveals that the addition of surfactant to lectin solution provokes an increase of R_H. In the case of pH 7.4, the size of the complexes increases to a larger extent that at pH 5. The aggregation of lectin is probably induced by the binding of MEGA-20 between different Con A molecules. Clearly this aggregation is more extended at pH 7.4. The

measured hydrodynamic radius of pure Con A at pH 7.4 and pH 5 were 4.9±0.3 nm and 4.0±0.4 nm, respectively. These values agree well with those previously published [45].

3.5. CD

Circular dichroism in the far UV region is one of the best spectroscopic techniques to determine the change in secondary structural contents of proteins after the binding of ligands. To get a clear image of how the conformation of lectin was affected by MEGA10 binding, CD measurements on free Con A, as well as in the presence of surfactant at both pHs were performed (see Figure 9). As can be seen, the native lectin spectrum is clearly different for pH 7.4 and pH 5. This is expected if one has in mind that the Con A forms tetramers at pH 7.4, whereas the structure is dimeric at pH 5. The plots are characterized by a broad negative trough centered at 223 nm for acid pH and at 225 nm for physiological pH. This kind of CD spectrum is typical for proteins rich in β-sheet structure [46]. In fact, the three-dimensional structure of monomeric Con A presents an antiparallel β-sandwich structure comprising a six-stranded flat "back" β-sheet, a seven-stranched curved "front", and a five-stranched "top" β-sheet roofing the other two [33]. CD spectrums of lectin obtained from different seeds also present a minimum peak at around 225 nm [47-49]. When MEGA10 was added to the protein solution, the magnitude of ellipticity (MRE) decreased, suggesting that Con A conformation had changed. The spectral pattern change is less pronounced at pH 5. This observation indicates a weaker change on the protein conformation at acid pH than at physiological pH after binding with MEGA10. This is in line with the results of quenching and time resolved fluorescence presented in previous sections. Thus, MEGA10 only slightly altered the secondary structure of the protein.

4. Conclusions

MEGA10 binding to Con A was revealed by the gradually decrease in fluorescence intensity of lectin upon surfactant addition. The surfactant affinity to protein is higher at pH 7.4 than at pH 5. Analysis of quenching data shows that the major proportion of Trp residues is buried and not available to surfactant. The sugar-binding site is probably not close to tryptophanyl groups. Thermodynamic parameters (ΔG^0, ΔH^0 and ΔS^0) were all negative, showing that association was spontaneous, and that hydrogen bonds and van der Waals forces are the predominant forces in stabilizing Con A-MEGA 10 complex. Time-resolved fluorescence studies confirm the binding of MEGA10 to Con A. The agglutination of Con A in the presence of MEGA10, assessed by DLS experiments, confirms the binding of the surfactant on lectin. The observed size increments were more substantial at physiological pH than at pH 5. At pH 5, the CD spectra obtained in the presence of MEGA10 is only slightly different from the one corresponding to the native Con A state, whereas a significant difference was observed at pH 7.4. Thus, the presence of surfactant at pH 5 does not seem to induce relevant conformational alterations in lectin.

5. Acknowledgements

This work has been sponsored by the MAT2015-62644-C2-1-R and MAT2015-62644-C2-2-R projects

References

[1] Y. Min, J.M. Caster, M.J. Eblan, A.Z. Wang, Clinical Translation of Nanomedicine, Chem. Rev, 115 (2015) 11147-11190.

[2] D. Peer, J.M. Karp, S. Hong, O.C. Farokhzad, R. Margalit, R. Langer, Nanocarriers as an emerging platform for cancer therapy, Nat. Nanotech, 2 (2007) 751-759

[3] H. Maeda, The enhanced permeability and retention (EPR) effect in tumor vasculature: the key role of tumor-selective macromolecular drug targeting, Adv. Enzyme Regul. 41 (2001) 189-207

[4] A. David, Carbohydrate-based biomedical copolymers for targeted delivery of anticancer drugs, Israel J. Chem. 50 (2010) 204-219

[5] I. Harbi, B. Aljaeid, K.M. El-Say, A. S. Zidan, Glycosylated Sertraline-Loaded liposomes for brain targeting: QbD study of formulation variabilities and brain transport, PharmSci. Tech. 17 (2016) 1404-1420

[6] G.P. Adams, L.M. Weiner, Monoclonal antibody therapy of cancer, Nat. Biotechnol. 23 (2005) 1147-1157

[7] M. Yamamoto, K. Ichinose, N. Ishii, T. Khoji, K. Akiyoshi, N. Moriguchi, J. Sunamoto, T. Kanematsu, Utility of liposomes coated with polysaccharide bearing 1-amino-lactose as targeting chemotherapy for AH66 hepatoma cells, Oncol. Rep. 7 (2000) 107-118

[8] J. Park, L.H. Rader, G.B. Thomas, E. J. Danoff, D.S. English, P. DeShong, Carbohydrate-funcionalized catanionic surfactant vesicles: preparation and lectin-binding studies, Soft Matt. 4 (2008) 1916-1921

[9] R. Lotan, Y. Matsushita, D. Ohannesian, D. Carralero, D.M. Ota, K.R. Cleary, G.L. Nicolson, T. Irimura, Lactose-binding lectin expression in human colorectal carcinomas. Relation to tumor progression, Carbohydrate Research 213 (1991) 47-57

[10] C. Bies, C.M. Lehr, J.F. Woodley, Lectin-mediated drug targeting: history and applications, Adv. Drug. Del. Rev. 56 (2004) 425-435

[11] F. Gabor, E. Bogner, A. Weissenboeck, M. Wirth, The lectin-cell interaction and its implications to intestinal lectin-mediated drug delivery, Adv. Drug Deliv. Rev. 56 (2008) 459-480

[12] J.A. Molina-Bolívar, C. Carnero Ruiz, Sugar-Based Surfactants: Fundamentals and Applications, in C. Carnero Ruiz (Ed), CRC Press Boca Raton, 2009

[13] M. Imran, M.R. Shah, F. Ullah, S. Ullah, A.M.A. Elhissi, W. Nawaz, F. Ahmad, A. Sadiq, I. Ali, Glycoside-based niosomal nanocarriers for enhanced in-vivo performance of Cefixine, Int. J. Pharm. 505 (2016) 122-132

[14] J. Feng, C. Lin, H. Wang, S. Liu, Gemini dodecyl O-glucoside-based vesicles as nanocarriers for catechin laurate, J. Func. Foods, 32 (2017) 256-265

[15] M. Salim, O.K. Abou-Zied, H. U. Kulathunga, A. Baskaran, U.R. Kuppusamy, R. Hashim, Alkyl mono- and di-glucoside sugar vesicles as potential drug delivery vehicles: detecting drug release using fluorescence, RSC Adv. 5 (2015) 55536-55543

[16] R. Muzzalupo, L. Tavano, C. La Mesa, Alkyl glucopyranoside-based niosomes containing methotrexate for pharmaceutical applications: Evaluation of physic-chemical and biological properties, Phar. Nano. 458 (2013) 224-229

[17] J. E. K. Hildreth, N-D-Gluco-N-methylalkanamide compounds, a new class of non-ionic detergents for membrane biochemistry, Biochem. J. 207 (1982) 363-366

[18] C. Carnero Ruiz, J. M Hierrezuelo, J. Aguiar, J. M. Peula-García, Physicochemical studies on the interaction between N-decanoyl-N-methylglucamide and bovine serum albumin, Biomacromolecules, 8 (2007) 2497-2503

[19] H. Lis, N. Sharon, in: A. Marus (Ed), The Biochemistry of Plants, vol 6, Academic Press, New York, 1981, pp 371-447

[20] M.V.R. Rao, M. Atreyi, M.R. Rajeswari, Fluorescence studies on concanavalin-A, J. Biosci. 6 (1984) 823-828

[21] S.M. Kelly, T.J. Jess, N.C. Price, How to study proteins by circular dichroism, Biochim. Biophys. Acta 1751 (2005) 119-139

[22] V.K. Sonu, M. M. Islam, A. B. Gurung, A. Bhattcharjee, S. Mitra, Serum albumin interaction with xanthine drugs and nano-bio interfaces: A combined multi-spectroscopic and molecular modelling approach, J. Mol. Liq. 242, 2017, 919-927

[23] Y.K. Reshetnyak, E.A. Burstein, Decomposition of protein tryptophan fluorescence spectra into long-normal components. II. The statistical proof of discreteness of tryptophan classes in proteins, Biophy. J. 81 (2001) 1710-1734

[24] J.A. Molina-Bolivar, C. Carnero Ruiz, F. Galisteo-Gonzalez, M. Medina-O´Donnell, A. Parra, Simultaneous presence of dynamic and sphere action component in the fluorescence quenching of human serum albumin by diphtholoylmaslinic acid. J. Luminescence, 178 (2017) 259-266

[25] R. Lakowicz, Principles of fluorescence spectroscopy, Third ed., Springer, New York, 2006

[26] C. Carrillo, D. Cordoba-Diaz, M. Cordoba-Diaz, T. Girbes, P. Jiménez, Effects of temperature, pH and sugar binding on the structures of lectins ebulin f and SELfd, Food Chemistry, 220 (2017) 324-330

[27] A. Narahari, M.J. Swamy, Tryptophan exposure and accessibility in the chitooligosaccharide-specific phloem exudate lectin from pumpkin (Curcubita maxima). A fluorescence study, Journal of Photochem. Photobiology B: Biology 97 (2009) 40-47

[28] R. Kenoth, M.J. Swamy, Steady-state and time-resolved fluorescence studies on *Trichosanthes cucumerina* seed lectin, Journal of Photochem. Photobiology B: Biology 69 (2003) 193-201

[29] D.H. Rao, L.R. Gowda, The d-galactose specific lectin of field bean (*Dolichos lablab*) seed binds sugars with extreme negative cooperativity and half-of-the-sites binding, Archives of Biochemistry and Biophysics, 524 (2012) 85-92

[30] O.A. Chaves, B. Mathew, D.Cesarin-Sobrinho, B. Lakshminarayanan, M. Joy, G. E. Mathew, J. Suresh, J.C. Netto-Ferrerira, Spectroscopic, zeta potential and molecular docking analysis on the interaction between human serum albumin and halogenated thienyl chalcones, J. Mol. Liq. 242 (2017) 1018-1026

[31] U.V. Katre, C.G. Suresh, M.I. Khan, S.M. Gaikwad, Steady state and time-resolved fluorescence studies of a hemagglutinin from Moringa oleifera, J. Fluoresc. 18 (2008) 479-485

[32] N. Moradi, M.R. Ashrafi-Kooshk, J. Chamani, D. Shackebaei, F. Norouzi, Separate and simultaneous binding of tamoxifen and estradiol to human serum albumin: spectroscopic and molecular modeling investigations, J. Mol. Liq. 249 (2018) 1083-1096

[33] P. Mandad, D.K. Manda, Localization en environment of different structural states of Concanavalin A, J. Fluoresc. 21 (2011) 2123-2132

[34] R. Pelley, P. Howorkitz, Fluorimetric studies of tryptophyl exposure in Concanavalin-A, Biochim. Biophys Acta 427 (1976) 359-363

[35] X. Zhang, H. Zhai, R. Gao, J. Zhang, Y. Zhang, X. Zheng, Study on the interaction between 4-thio-5-methyluridine and human serum albumin by spectroscopy and molecular modeling, Spectrochimica Acta Part A: molecular and biomolecular spectroscopy 121 (2014) 724-731

[36] J. Ma, Y. Liu, L. Chen, Y. Xie, L.Y. Wang, M.X. Xie, Spectroscopic investigation on the interaction of 3,7-dihydroxyflavone with different isomers of human serum albumin, Food Chemistry 132 (2012) 663-670

[37] J.A. Molina-Bolivar J.A. C. Carnero Ruiz, F. Galisteo-Gonzalez, M. Medina-O´Donnell, A. Parra, Energetics of albumin-disuccinylmaslinic acid binding determined by fluorescence spectroscopy, Fluid Phase Eq. 400 (2015) 43-52

[38] S.K. Pawar, P. Vavia, Efficacy interactions of PEG-DOX-N-acetyl glucosamine prodrug conjugate for anticancer therapy, Eur. J. Pharm. Biopharm. 97 (2015) 454-463

[39] R.D. Farina, R.G. Wilkins, Kinetics of interaction of some α- and β-D-monosaccharides with Concanavalin A, Biochim. Biophys. Acta, 631 (1980) 428-438

[40] P.D. Ross, S. Subramanian, Thermodynamics of protein association reactions: forces contributing stability, Biochemistry 20 (1981) 3096-3102

[41] J.M. Hierrezuelo, J.A. Molina-Bolívar, C. Carnero Ruiz. An energetic analysis of the phase separation in non-ionic surfactant mixtures: the role of the headgroup structure, Entropy 16 (2014) 4375-4391

[42] R.V. Watherman, L.L. Kiessling, Fluorescence anisotropy assays reveal affinities of C- and O-glycosides for Concanavalin A, J. Org. Chem. 61 (1996) 534-538

[43] Y. Xu, S.V. Oruganti, V. Gopalan, M.P. Foster, Thermodynamics of coupled folding in the interaction of Archaeal RNase P Proteins RPP21 and RPP29, Biochemistry, 51 (2012) 926-935

[44] B. Ojha, G. Das, The interaction of 5-(Alkoxy)naphathalen-1-amine with Bovine Serum Albumin and its effect on the conformation of protein, J. Phys. Chem. B, 114 (2010) 3979-3986.

[45] G.V. Deodhar, M.L. Adams, S. Joardar, M. Joglekar, M. Davidson, W.C. Smith, M. Mettler, S. A. Toler, F.K. Davies, S.K.R. Williams, B.G. Trewyn, Conserved activity of reassociated homotetrameric protein subunits released form mesoporous silica particles, Langmuir 34 (2018) 228-233

[46] J.M. Khan, M.S. Khan, M.S. Ali, N.A. Al-Shabib, R.H. Khan, Cetyltrimethylammonium bromide (CTAB) promote amyloid fibril formation in carbohydrate binding protein (concanavalin A) at physicological pH, RSC Adv. 2016, 6, 38100-38111

[47] R. Adar, N. Sharon, Mutational studies of the amino acid residues in the combining site of *Erythrina corallodendron* lectin, Eur. J. Biochem. 239 (1996) 668-674

[48] E.H.E. Konozy, E.S. Bernardes, C. Rosa, V. Faca, L.J. Greene, R.J. Ward, Isolation, purification, and physicochemical characterization of a D-galactose-binding lectin from seeds of *Erythrina speciosa*, Archives of Biochemistry and Biophysics, 410 (2003) 222-229

[49] P. Yadav, G. Shahane, S. Ramasamy, D. Sengupta, S. Gaikwad, Structural-functional insights and studies on saccharide binding of *Sphora japonica* seed lectin, Int J. of Biological Macromolecules, 91 (2016) 75-84

Table and Figure captions

Table 1. Binding constant (K_a) and thermodynamic parameters for Con-MEGA10 complex at pH 7.4 and pH 5

Table 2. Fluorescence lifetime decay analysis of Con A upon MEGA10 addition at pH 7.4

Table 3. Fluorescence lifetime decay analysis of Con A upon MEGA10 addition at pH 5

Figure 1. The fluorescence quenching spectra of Con A in the presence of various concentrations of MEGA10 at [Con A]=11 μM and T=298 K: (A) pH 7.4, (B) pH 5.

Figure 2. Stern-Volmer plot for the binding of MEGA10 to Con A at pH 7.4 and pH 5

Figure 3. Plot of $I_0/\Delta I$ against 1/[MEGA10] at pH 7.4 and pH 5

Figure 4. Quenching data plotted according to Eq. 5 for the binding of MEGA10 to Con A at different temperatures. (A) pH 7.4; (B) pH 5

Figure 5. Plots of $\Delta G^0/T$ vs. T at pH 7.4 and pH 5

Figure 6. (A) Fluorescence decays of Con A in the absence and presence of 160 μM of MEGA10 together with the instrumental response function (IRF) at pH 7.4

The lines correspond to fits. (B) Plots of τ vs. concentration of MEGA10 at pH 7.4 and pH 5

Figure 7. Fluorescence anisotropy of Con A as a function of MEGA10 concentration at pH 7.4 and pH 5

Figure 8. Hydrodynamic radius of Con A-MEGA 10 complexes at a function of MEGA10 concentration at pH 7.4 and pH 5

Figure 9. CD spectra of Con A in the absence and presence of MEGA10 at pH 7.4 and pH 5. Molar ratio of 1:5

TABLE 1

	T (K)	K_a x10^{-3} (L mol^{-1})	ΔH^0 (kJ mol^{-1})	$T\Delta S^0$ (J mol^{-1} K^{-1})	ΔG^0 (kJ mol^{-1})
pH 7.4	298	22.9±0.8	-66.1±1.0	-41.3±1.0	-24.8±0.1
	305	10.3±0.4	-69.2±1.0	-45.8±1.0	-23.4±0.1
	310	7.9±0.3	-71.5±1.0	-48.4±1.0	-23.1±0.2
pH 5	298	7.6±0.2	-55.5±1.0	-33.4±1.0	-22.1±0.1
	305	4.8±0.2	-58.1±1.0	-36.6±1.0	-21.5±0.1
	310	3.1±0.1	-60.0±1.0	-39.3±1.0	-20.7±0.2

TABLE 2

[MEGA10] (µM)	τ_1 (ns)	α_1	τ_2 (ns)	α_2	τ_3 (ns)	α_3	χ^2
0	0.82	0.46	2.34	0.38	5.60	0.16	0.99
20	0.67	0.45	2.06	0.38	5.17	0.17	1.05
40	0.64	0.44	2.03	0.38	5.02	0.18	1.06
70	0.54	0.44	1.88	0.38	4.91	0.18	1.01
120	0.41	0.42	1.66	0.40	4.67	0.18	1.03
160	0.40	0.40	1.63	0.40	4.62	0.20	1.00

TABLE 3

[MEGA10] (μM)	τ_1 (ns)	α_1	τ_2 (ns)	α_2	τ_3 (ns)	α_3	χ^2
0	0.70	0.40	2.00	0.43	4.60	0.17	1.02
20	0.67	0.40	1.89	0.42	4.50	0.18	1.06
40	0.59	0.40	1.89	0.42	4.49	0.18	1.01
70	0.57	0.39	1.81	0.42	4.43	0.19	1.03
120	0.74	0.40	1.96	0.41	4.55	0.19	1.07
160	0.63	0.39	1.88	0.41	4.42	0.20	1.02

FIGURES

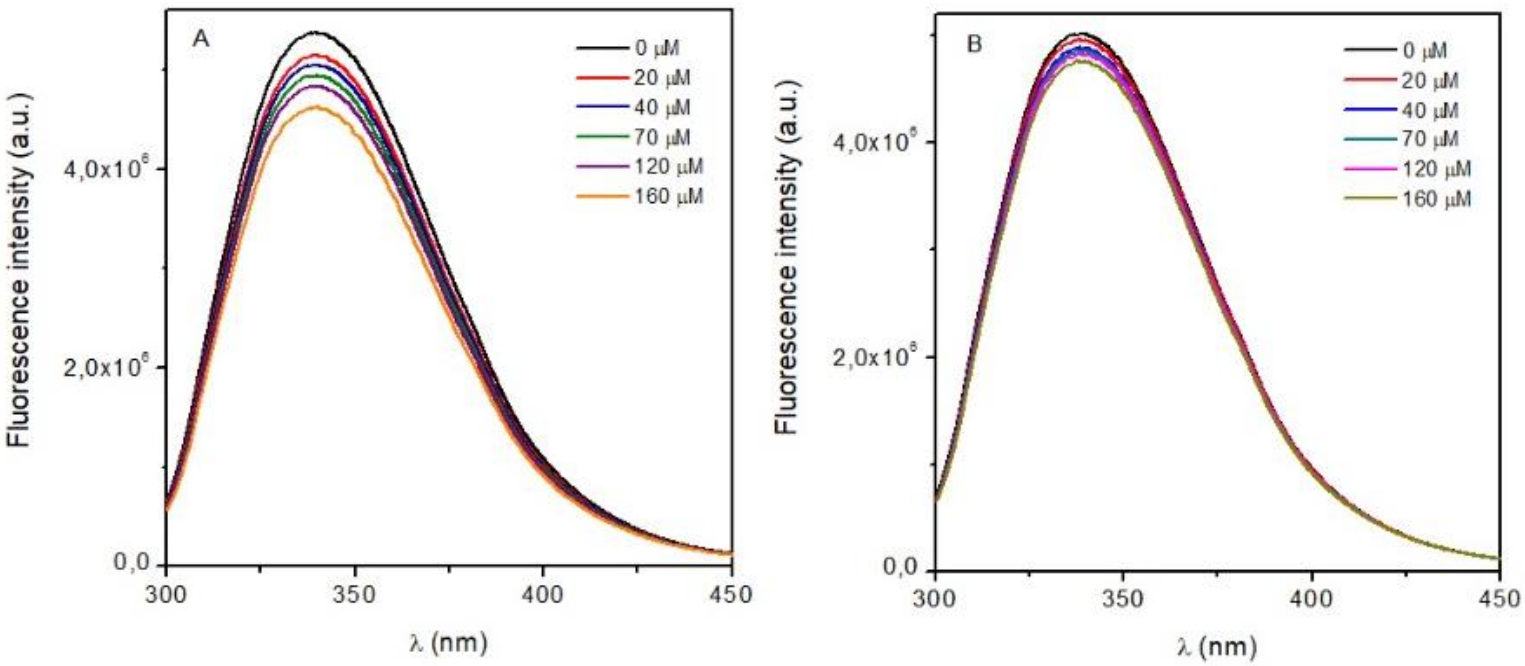

Figure 1

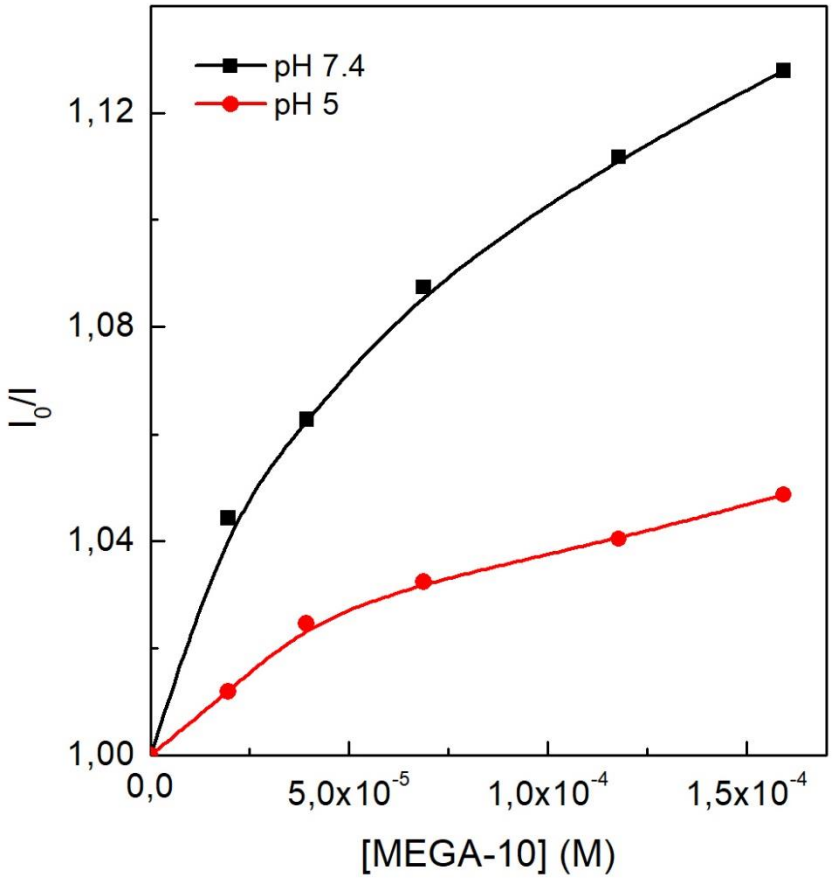

Figure 2

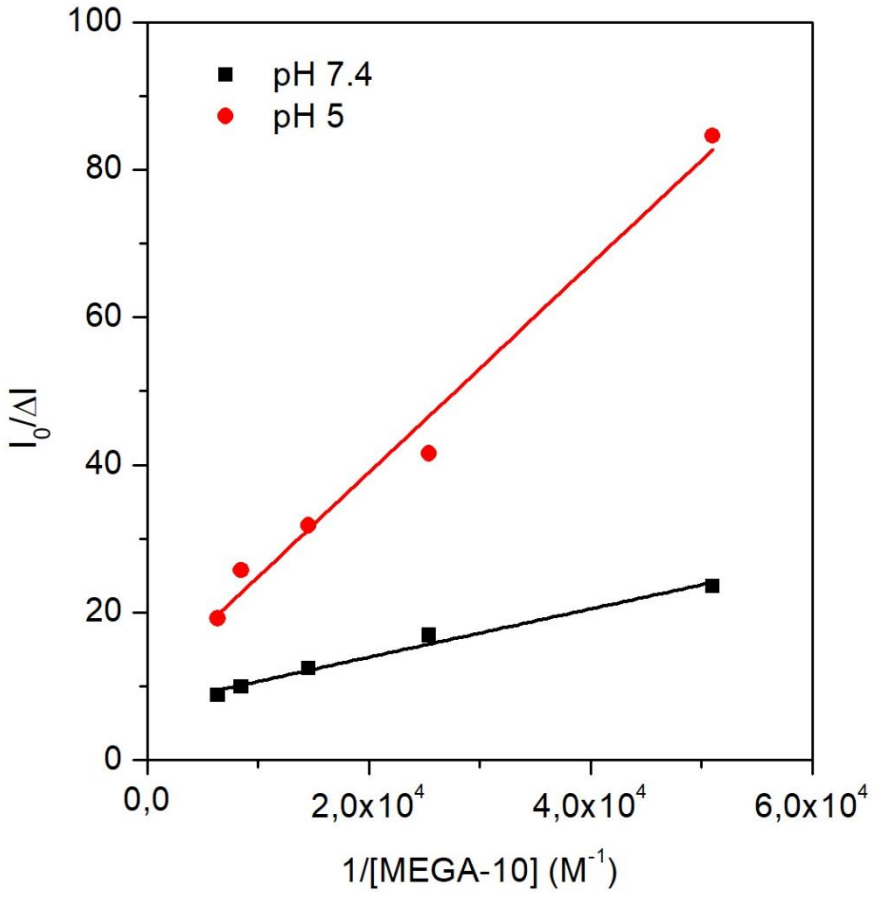
100
80
60
40
20
0
pH 7.4
pH 5
$I_0/\Delta I$
0,0
2,0x10^4
4,0x10^4
6,0x10^4
1/[MEGA-10] (M^{-1})

Figure 3

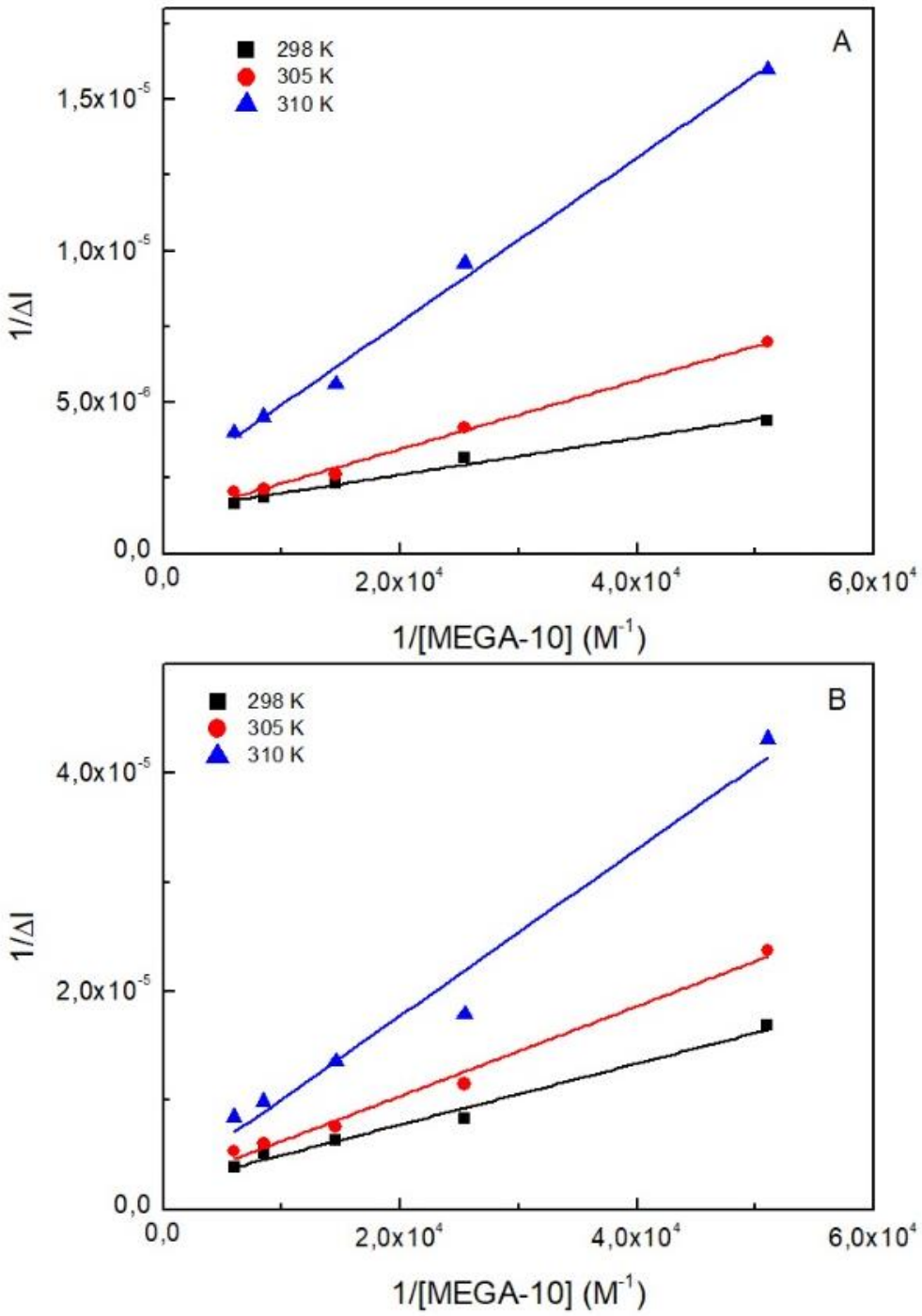
A
298 K
305 K
310 K
1,5x10-5
1,0x10-5
5,0x10-6
0,0
1/ΔI
0,0
2,0x10⁴
4,0x10⁴
6,0x10⁴
1/[MEGA-10] (M-1)
B
298 K
305 K
310 K
4,0x10-5
2,0x10-5
0,0
1/ΔI
0,0
2,0x10⁴
4,0x10⁴
6,0x10⁴
1/[MEGA-10] (M-1)

Figure 4

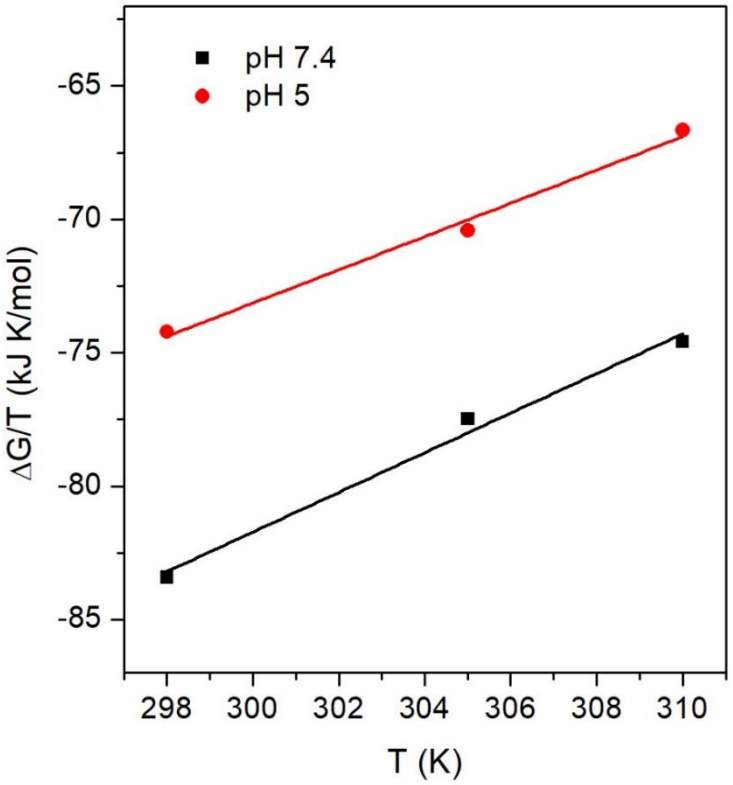

Figure 5

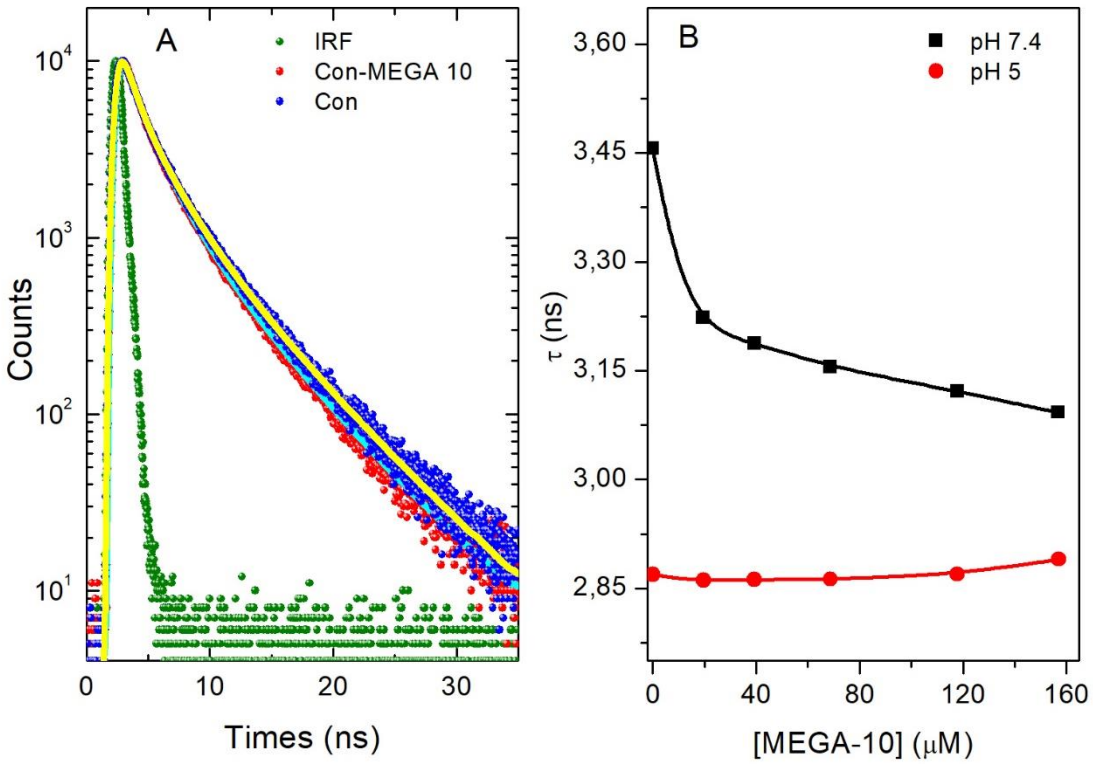

Figure 6

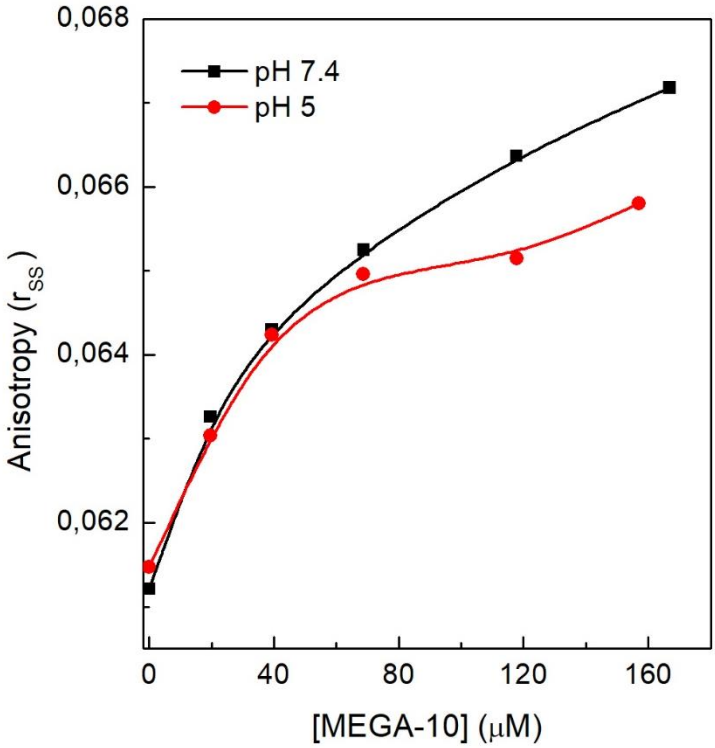

Figure 7

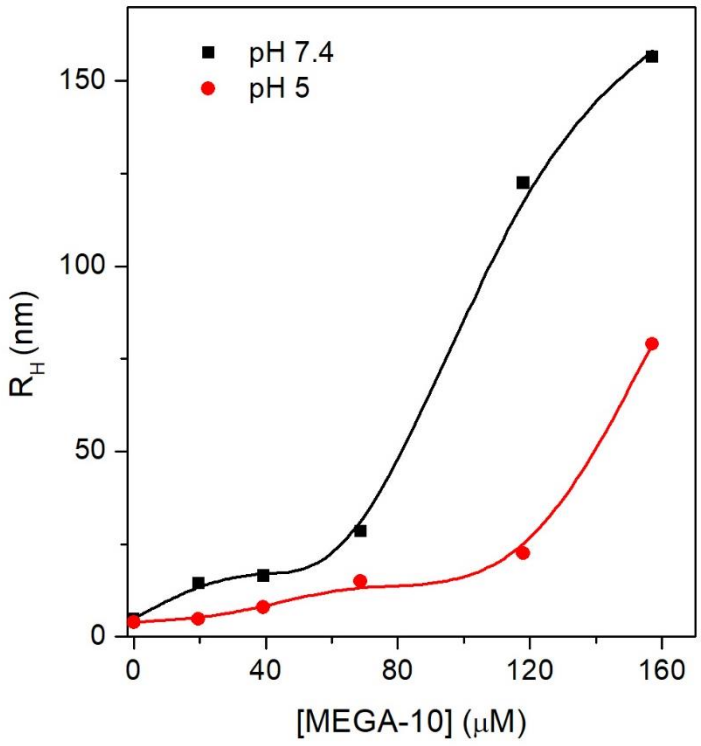

Figure 8

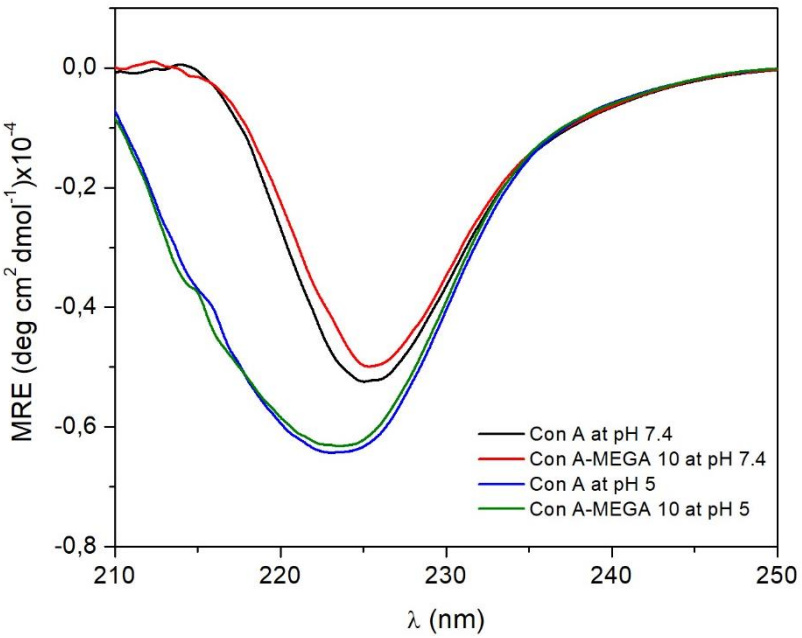
0,0
-0,2
-0,4
-0,6
-0,8
210
220
230
240
250
λ (nm)
MRE (deg cm2 dmol-1)x10-4
Con A at pH 7.4
Con A-MEGA 10 at pH 7.4
Con A at pH 5
Con A-MEGA 10 at pH 5

Figure 9